nature photonics

ARTICLES

PUBLISHED ONLINE: 28 JULY 2013 | DOI: 10.1038/NPHOTON.2013.188

Ultrathin, highly flexible and stretchable PLEDs

Matthew S. White[1]*, Martin Kaltenbrunner[2,3,4], Eric D. Głowacki[1], Kateryna Gutnichenko[1], Gerald Kettlgruber[4], Ingrid Graz[4], Safae Aazou[5,6], Christoph Ulbricht[7], Daniel A. M. Egbe[1], Matei C. Miron[8], Zoltan Major[8], Markus C. Scharber[1], Tsuyoshi Sekitani[2,3], Takao Someya[2,3], Siegfried Bauer[4] and Niyazi Serdar Sariciftci[1]

We demonstrate ultrathin (2 μm thick) red and orange polymer light-emitting diodes with unprecedented mechanical properties in terms of their flexibility and ability to be stretched. The devices have a luminance greater than 100 cd m^{-2}, sufficient for a variety of optoelectronic applications including indoor displays. They can be operated as free-standing ultrathin films, allowing for crumpling during device operation. Furthermore, they may be applied to almost any surface whether rigid or elastomeric, and can withstand the associated mechanical deformation. They are shown to be extremely flexible, with radii of curvature under 10 μm, and stretch-compatible to 100% tensile strain. Such ultrathin light-emitting foils constitute an important step towards integration with malleable materials like textiles and artificial skin.

The emerging field of electronics integration places new physical requirements on electronic components. Integration directly into or onto malleable materials such as textiles or biological tissues is of increasing interest for applications spanning the medical, safety, security, infrastructure and communication industries, among many others. The unique requirement imposed in this field is that the electronics must be highly flexible to survive the mechanical deformation of the malleable host material[1–8]. Some specific requirements include flexing, with a radius of curvature significantly smaller than 1 mm, and the ability to undergo stretching and compression to various degrees. As there are no truly stretchable electronics, the most successful approach to meet the stretching requirement is to use flexible electronics, allowing orthogonal flexing to mediate the stretching and compression strain[1–3,7,9–16].

In this Article, we combine highly flexible conducting polymers, semiconducting polymers and thin metal layers to form fully functional polymer-based organic light-emitting diodes (PLEDs) on ultrathin, 1.4 μm polyethylene terephthalate (PET) foil substrates. Because the materials have a relatively high critical strain, and the substrate is extremely thin, the devices are operable under extreme flexing conditions with radii of curvature under 10 μm. We demonstrate two colours of ultrathin PLEDs—orange and display-specification red—both with display operational luminance greater than 100 cd m^{-2}. These can be operated as free-standing foils or as conforming layers on arbitrary surfaces. In particular, we demonstrate the first stretch-compatible PLEDs in continuous operation under 100% stretching strain while adhered to an elastomeric tape.

Results

A layer schematic of the ultrathin PLEDs is shown in Fig. 1a, with the thickness of each layer drawn to scale. The total thickness of the substrate, electrodes and light-emitting semiconducting polymer layers is 2 μm. The substrate, a 1.4-μm-thick PET foil (Mylar 1.4 CW02), is a commercially available, commodity-scale material used as a foil capacitor dielectric. The transparent electrode is also a commercially available poly(3,4-ethylenedioxythiophene):poly(styrenesulphonate) (PEDOT:PSS) formulation (Clevios PH1000). An anthracene-containing poly(*p*-phenylene-ethynylene)-*alt*-poly(*p*-phenylene-vinylene) (PPE-PPV) derivative with a statistical distribution of linear octyloxy and branched 2-ethylhexyloxy side groups (AnE-PV*stat*) is used as a semiconducting, red light-emitting polymer. The chemical structure is shown in Fig. 1a[17]. This material is highly luminescent, with a red colour, and is known to have good electron and hole transport[18,19]. For orange-emitting PLEDs, the well-known poly[2-methoxy-5(3,7-dimethyloctyloxy)]-1,4-phenylenevinylene (MDMO-PPV) is deposited to a thickness of 225 nm. Finally, a LiF/Al electrode forms the back contact.

The luminance–voltage and current–voltage characteristics of the best AnE-PV*stat*- and MDMO-PPV-based ultrathin PLEDs are shown in Fig. 1b. We have fabricated 40 or more ultrathin PLEDs of each colour with 100% pixel success, although with significant pixel-to-pixel variation associated with film thickness fluctuations. The AnE-PV*stat* devices show a luminance of 32.7 ± 23.8 cd m^{-2} at 9 V, with a highest luminance of 113 cd m^{-2}. They have a power efficiency of 0.026 ± 0.017 cd A^{-1} and external quantum efficiency (EQE) of 0.08 ± 0.04%. The MDMO-PPV devices have a luminance at 9 V of 76.2 ± 30.3 cd m^{-2}, with a highest luminance of 122 cd m^{-2}. They have a power efficiency of 0.17 ± 0.06 cd A^{-1} and EQE of 0.44 ± 0.12%. They are fully functional PLEDs, with reasonable operating conditions of <5 V turn on voltage and three orders of magnitude diode rectification. Their operational lifetime depends strongly on the operational intensity due to heat management. However, at low intensities, they have been operated for several hours at partial duty cycle with no observed degradation.

For reference, we fabricated the same structure on indium tin oxide (ITO)-coated glass substrates, using a 25-nm-thick interlayer of the CLEVIOS P formulation PEDOT:PSS. The results are

[1]Johannes Kepler University, Linz Institute for Organic Solar Cells (LIOS), Department of Physical Chemistry, Altenbergerstrasse 69, 4040 Linz, Austria, [2]The University of Tokyo, Electrical and Electronic Engineering and Information Systems, 7-3-1 Hongo, Bunkyo-ku, Tokyo 113-8656, Japan, [3]Exploratory Research for Advanced Technology (ERATO), Japan Science and Technology Agency (JST), 2-11-16, Yayoi, Bukyo-ku, Tokyo 113-0032, Japan, [4]Johannes Kepler University, Soft Matter Physics, Altenbergerstrasse 69, 4040 Linz, Austria, [5]Laboratory for Solid State Physics, Interfaces and Nanostructures, Physics Department, University of Liege, Liege, Belgium, [6]Laboratory of Instrumentation, Measure and Control, Physics Department, Chouaïb Doukkali University, El Jadida, Morocco, [7]MEET Battery Research Center, Institute of Physical Chemistry, University of Muenster, Correnstrasse 46, 48149 Muenster, Germany, [8]Johannes Kepler University, Institute of Polymer Product Engineering, Altenbergerstrasse 69, 4040 Linz, Austria. *e-mail: matthew.white@jku.at

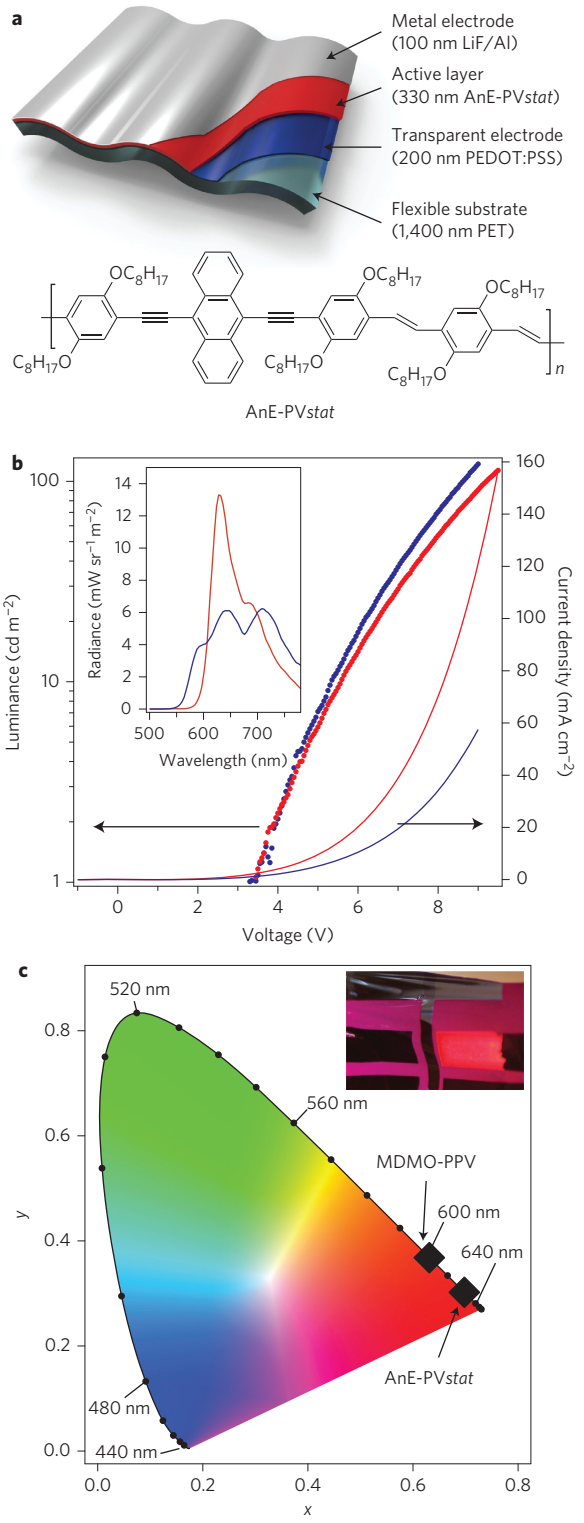

Figure 1 | Electrical and optical characterization of ultrathin PLEDs. **a**, Compositional schematic of devices with each layer thickness drawn to scale. The schematic shows periodic bending with a radius of curvature of ~5 μm for reference. The chemical structure of AnE-PV*stat* is shown below. **b**, Luminance–voltage (left axis, dots) and current–voltage (right axis, lines) characteristics of AnE-PV*stat* (red) and MDMO-PPV (blue) PLEDs. Radiance of the devices operated at 9.5 V (113 cd m^{-2}) and 9 V (122 cd m^{-2}), respectively. **c**, CIE 1931 *x*–*y* chromaticity diagram showing the perceptibly red colour of the AnE-PV*stat* emission and the orange colour of the MDMO-PPV. Inset: photograph showing a free-standing AnE-PV*stat* ultrathin PLED (~3 mm × 6 mm) driven at 25 mA cm^{-2}.

presented in Supplementary Fig. S1, and are approximately the same as for the ultrathin devices taking into account film thickness fluctuations. ITO has a significantly lower sheet resistance (15 Ω sq^{-1}) than the conductive PEDOT:PSS (135 Ω sq^{-1}) electrode. However, ITO is undesirable for use in large-area, flexible electronics because of cost and availability considerations, as well as the brittle nature of the ternary oxide[20,21].

The bandgap of the AnE-PV*stat* polymer is known to be ~2 eV (ref. 19). Not surprisingly, the resulting PLEDs are red in colour. More specifically, the radiance (Fig. 1b, inset) spans 600 to 750 nm, peaking at 630 nm. According to the CIE 1931 standard colour-matching functions, this is represented by the *x*,*y* chromaticity coordinates (0.698,0.302). As seen in Fig. 1c, this correlates to a perceptibly red colour, suitable for display use. The MDMO-PPV-based ultrathin PLEDs emit at wavelengths longer than 550 nm. The additional green contribution to the emission yields an orange colour with resulting chromaticity coordinates (0.631,0.368). This concept may be applicable for any colour, provided a balance of film thickness, layer uniformity, carrier mobility and surface roughness can be achieved. Additional information relating to the chromaticity calculations is presented in Supplementary Fig. S2. Notably, a red emitter will have lower luminance (Y) than a green emitter with the same radiance due to the overlap with the sensitivity of the human eye. The luminance required for displays varies by application, with 100–200 cd m^{-2} common for indoor monitors and 500–1,000 cd m^{-2} desired for mobile applications[22,23]. Both colours of ultrathin PLEDs presented here demonstrate a luminance greater than 100 cd m^{-2}, approaching the indoor display requirement range. PLEDs with higher luminance, over 1,000 cd m^{-2}, have been demonstrated using the same electroluminescent polymers, but this is not achievable to date on ultrathin substrates because of power and heat management considerations[19].

The ultrathin PLEDs are fabricated while the PET foil is loosely adhered to a polydimethylsiloxane (PDMS)-coated rigid glass support to ease processing. Initial electrical and optical characterization is performed before removal from the support. The PLEDs can then be simply peeled away from the support, operated as free-standing foils, and re-applied to any PDMS-coated or otherwise adhesive surface. Accordingly, they function as both free-standing and surface-conforming thin-film electronics.

Discussion

The primary goal in using such a thin substrate is to maximize the flexibility of the devices. To first order, the surface bending strain on the active electronic device can be expressed as $S = h/2R$, where h is the thickness of the film and R is the bending radius of curvature. Thus, any reduction in h corresponds to the same reduction in R without subjecting the sensitive active components to additional stress. In the case of these ultrathin PLEDs, it should be noted that this is only an approximation. A more detailed formula accounting for the different materials in the stack is discussed in the Supplementary Methods. However, we can use the first-order approximation to estimate the flexibility of the ultrathin devices. It has been shown that polymer-based electronics can show critical bending radii of ~1 mm with a substrate thickness of 125 μm (ref. 24). We therefore expect that a reduction in substrate thickness to 1.4 μm will allow for a bending radius of ~10 μm. Bending with such a small radius will be required for integration with textiles and artificial skin-type applications, given that the electronic components must survive deformation at joints like knuckles and elbows. This is essential if the foil-based electronics are to reversibly undergo folding, wrinkling, crumpling and twisting deformations, without catastrophic failure.

As a first demonstration that these ultrathin PLEDs can withstand such extreme deformation, we suspended the foil between two glass slides. One of the glass slides was then moved closer to

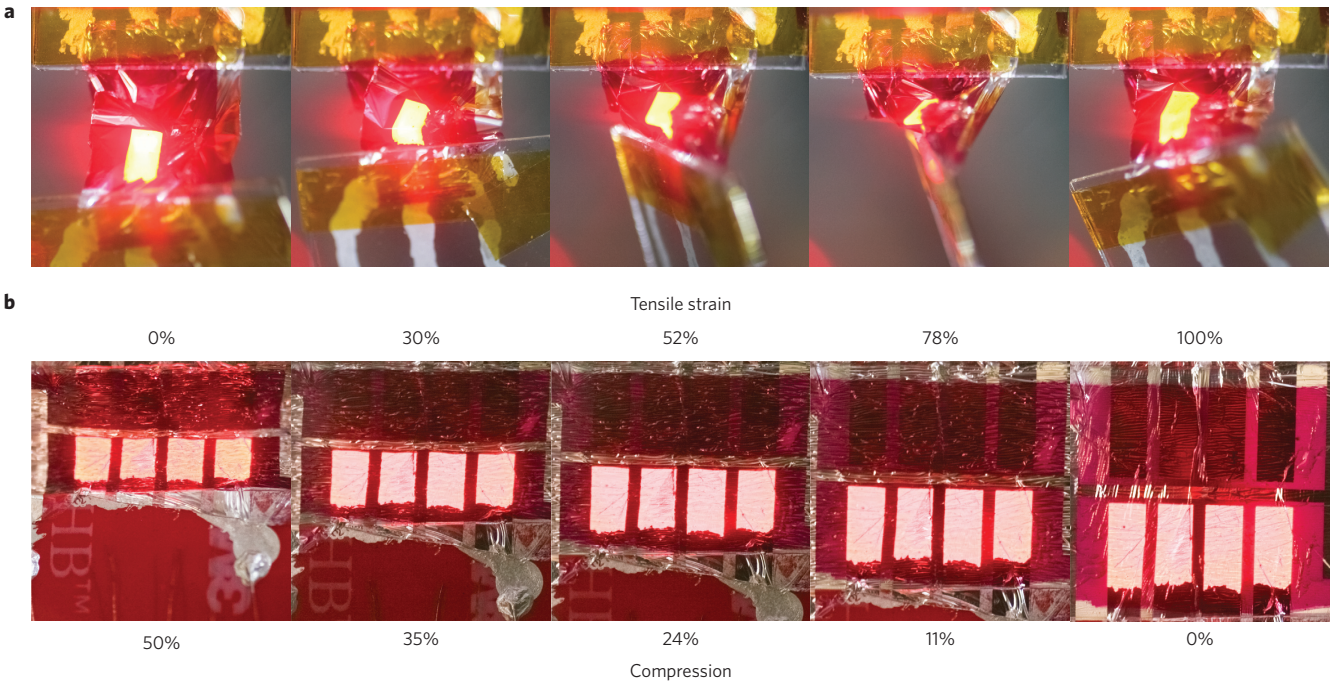

Figure 2 | Demonstrations of extreme deformation attainable with ultrathin PLEDs. a, Images of a free-standing ultrathin PLED operating during crumpling. The device is suspended between two pieces of glass that are moved closer together and simultaneously twisted by 90°. **b**, Images of an ultrathin PLED adhered to a prestrained elastomer tape. The images from left to right represent the wrinkled PLED (unstrained elastomer) state being stretched to the flat PLED (stretched elastomer) state. These are selected from 48 such images representing various stages of compression and stretching, which are compiled into Supplementary Movie S2. Each pixel is ~3 mm × 6 mm.

the other, decreasing the gap and allowing the foil to buckle. Simultaneously, the slide was twisted by 90°, resulting in an overall crumpling and twisting of the device. The PLEDs were operated continuously under this crumpling motion, and demonstrative photographs of the action are shown in Fig. 2a. Supplementary Movie S1 shows two demonstrations of ultrathin PLEDs operating in the free-standing foil configuration. The PLED was first suspended between two pieces of more rigid plastic and crumpled, similar to Fig. 2a. The second portion of the movie shows the PLED being crumpled by hand.

With such extremely flexible electronics, one can begin to imagine compatibility with stretching. Stretchable electronics is a topic of great current interest[1,7,9,11–16,25–36]. To borrow terminology from polymer science, one could consider three types of material response to deformation: brittle, tough and elastomeric. These three types of material show characteristic behaviour under strain ($\varepsilon = \Delta L/L_0$). Brittle deformation would result in total failure beyond a typically low critical strain. Tough materials would show irreversible deformation beyond a critical strain, with total failure at a much higher strain. Elastomeric deformation is characterized by reversible strain to hundreds of percent. Most conventional electronics undergo brittle deformation under very small strain, so any reversible elastomeric deformation, even on the order of 10%, is considered a successfully stretchable electronic device[1,7,11].

Stretchable polymers, such as polybutadiene, derive their elastomeric nature from bending and reorganization at the atomic and molecular scales. Materials used in electronics, even conducting and semiconducting polymers, do not share this property. Stretchable electronics incorporate bending and reorganization at larger scales to accommodate the same tensile strain. Successful approaches range from flexible interconnect ribbons between rigid active components to nanotube/nanowire networks embedded in elastomeric polymers[1,7,9,12,25,27,32–36]. The latter technique resembles intrinsically stretchable polymers much more closely. However, all successful techniques rely on the same fundamental principles of highly flexible electronic components integrated with elastomeric host materials.

The ultrathin PLEDs presented in this work are an ideal candidate for stretch compatibility. Realizing stretchable PLEDs requires two very simple additional processing steps. An adhesive elastomer (3M VHB) is prestretched to a desired total strain. The ultrathin PLED is then peeled off the glass preparation support and pressed onto the prestretched elastomer. A diagram showing the stretching apparatus and specifying the compression and tensile strain definitions is presented in Supplementary Fig. S3. In this work we use 100% prestrain, but up to 400% has been demonstrated using similar techniques for solar cells[26]. As the elastomer is relaxed to its unstrained state, the PLED forms a random network of folds to accommodate the compression strain. By doing so, the PLED maintains its performance at nearly the same level as in its flat state. The current–voltage traces of an AnE-PV*stat*-based PLED in the flat and 30% compressed states are shown in Supplementary Fig. S4, and are virtually indistinguishable. The radiance of the same PLED under the same conditions is also shown in Supplementary Fig. S4, and it can be seen that by detecting a wider range of emission angles relative to the surface normal, interference effects tend to minimize. The formation and utility of such wrinkles, folds and delaminations upon compression is the subject of several independent investigations[37–41].

The images shown in Fig. 2b show how the PLED can be stretched with up to 100% tensile strain. Compression and stretching of this scale can be repeated many times without damage to the device. Still images of two compression/stretching cycles to 40% and 50% compression were compiled into a stop-motion movie, which is available as Supplementary Movie S2. The stages of compression shown in the movie are plotted in Fig. 3a. Further analysis of the images shows that there are an average of 25 folds (peak-to-peak) in the length of each PLED. The number of peaks does not increase upon compression; instead, the peak spacing reduces. This information can be used to model an ideal compression of the film,

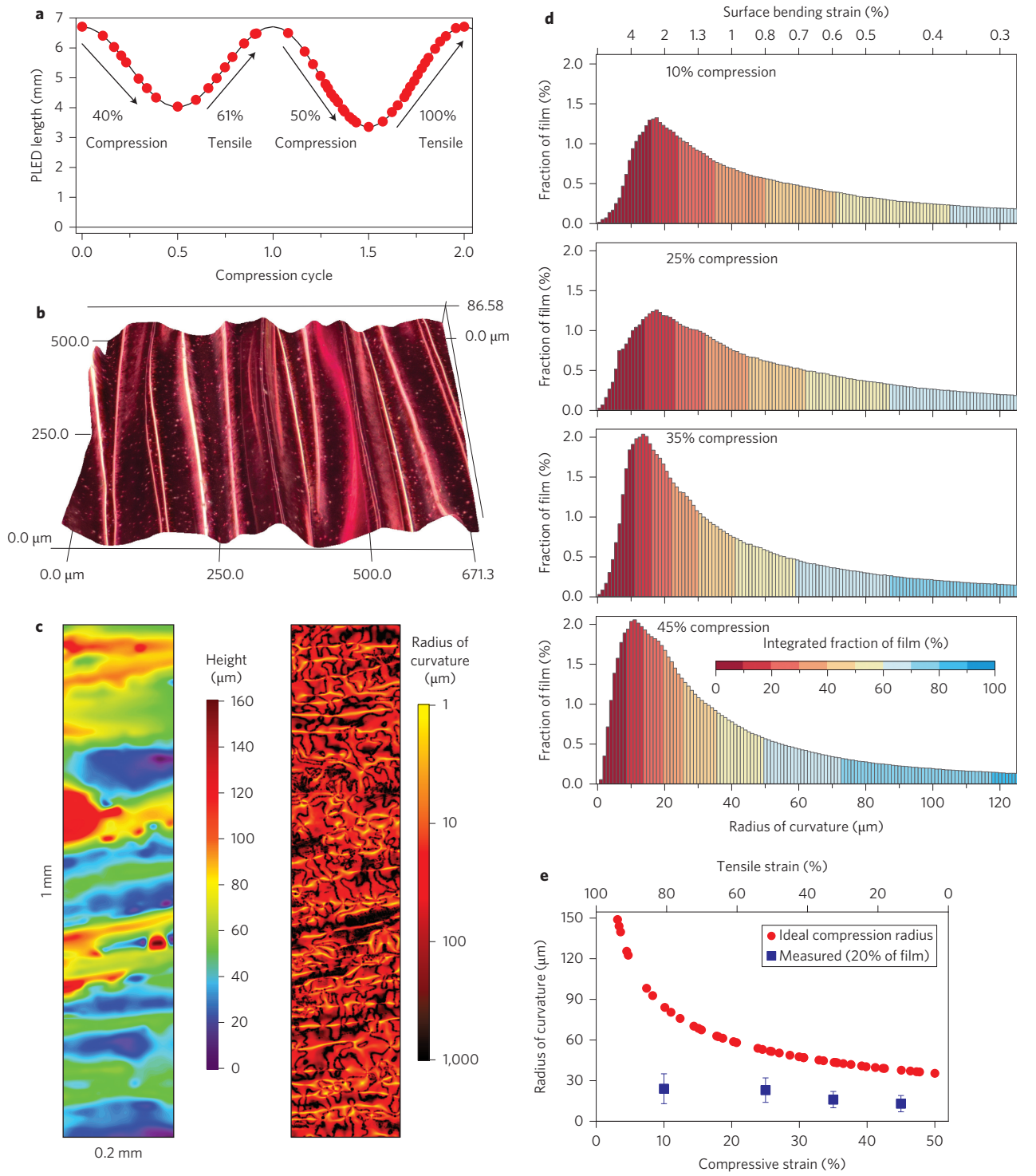

Figure 3 | Wrinkling and folding of PLED films during compression. **a**, Length of the PLED during two compression cycles (shown in Supplementary Movie S2). **b**, Three-dimensional digital optical micrograph of the PLED film. **c**, Height map of the 45% compressed film (left) and the corresponding radius of curvature map with logarithmic colour scale (right). **d**, Histograms of the radius of curvature maps for 10, 25, 35 and 45% compression. The colour scale represents the integrated fraction of the film with bending radius less than or equal to that value. Top axis shows the estimated bending strain at the surface of the aluminium electrode. **e**, Radius of curvature at each stage of compression. Red circles represent the radius for compression under minimal strain. Blue squares represent the 20% integrated fraction of the film in the histograms in **d**. Error bars represent the bin width from the 20–30% integrated fractions.

that is, compression that would theoretically cause the least damage to the PLED by eliminating sharp creases. To do this we use the average peak-to-peak distance, assuming tangentially connected arc segments of constant radius and the constraint that the total length of the PLED does not change. A schematic showing the ideal compression is presented in Supplementary Fig. S5, and further discussion is provided in the Supplementary Methods. The resulting 'ideal' radius of curvature for each stage of compression is plotted in Fig. 3e (red circles).

Digital optical micrographs of the ultrathin films under four discrete stages of compression were taken, using a vertical scan of the focal plane to map the height profile. The example in Fig. 3b shows a

PLED compressed to ~45%. Full height profile maps for 10, 25, 35 and 45% compression are shown in Supplementary Fig. S6. Utilizing the three-dimensional map of the film surface, we can calculate a radius of curvature for each point in the image. Both the height map and calculated radius of curvature map for a 0.2 mm × 1 mm strip of the film under 45% compression are shown in Fig. 3c. The yellow coloured areas in the radius map represent locations with a radius of curvature less than 10 μm. There are very few isolated points with radii less than 5 μm. Histograms of the radius map for all four stages of compression are shown in Fig. 3d. It is evident that, even under small compression, there is already a network of folds with very tight bending radii. This indicates that the film deforms far from the 'ideal compression' model (Supplementary Fig. S5). The measured values for radius of curvature are plotted in Fig. 3e. We plot the value for which 20% of the film area is bent to a smaller radius, as indicated by the colour scale in the histograms of Fig. 3d. The error bars represent the bin width occupied between the 20% and 30% integrated film fraction. Quantitative mechanical analysis of ultrathin PLEDs with the layer structure shown in Fig. 1a was performed, and the results are shown in Supplementary Fig. S7. A static implicit analysis shows the strain localization in the film bent to a radius of 30 μm, and a dynamic explicit simulation shows the formation of a seemingly random network of folds in the time domain.

These ultrathin PLEDs are shown to be stretch-compatible, to a degree approaching the conventional definition of elastomeric deformation (~200% tensile strain). This is the first report of a stretchable PLED, and warrants comparison to the two previous reports of other stretchable organic light-emitting devices. In 2011, Yu and colleagues utilized electrodes consisting of a network of conducting carbon nanotubes embedded in a polymer host to construct polymer-based light-emitting electrochemical cells (PLECs)[25]. When heated above the glass-transition temperature of the host polymer, the electrodes behave like rubbery elastomers. On heating to 70 °C, it was shown that the PLECs can be stretched to 45% tensile strain. This elegant approach utilizes reorganization of the nanotube network at the 1 μm scale, whereas the ultrathin PLEDs presented here deform at the 10 μm scale. Sekitani and colleagues have demonstrated a stretchable active-matrix organic LED (OLED) display, where the stretching occurs primarily in the interconnect area between rigid OLED pixels[9].

The ultrathin technology presents several distinct advantages over previous stretchable organic light-emitting devices. Because the devices are extremely flexible, it is no longer necessary to control the locus of the bending within a large-area electronic device. Interconnects and PLEDs can both accommodate tensile strain. LEDs and LECs also have distinct advantages and disadvantages that should be considered for various applications[42]. Of relevant concern here are the slow response and bipolar emission/*I*–*V* characteristics of LECs, which render them incompatible for use in display technology. In Supplementary Movie S3, we show an AnE-PV*stat*-based PLED undergoing 30% compression and stretching while individual pixels are addressed at 4 Hz. The same system has been used to address pixels at up to 50 Hz. Stretching at room temperature is also advantageous for most standard applications. Finally, constructing a stretchable light emitter from an ultrathin PLED is a simple peel-and-stick process.

Perhaps the most important advantage of this ultrathin technology is its ease of processing. Because the substrate foil naturally adheres, via van der Waals bonding, to a PDMS-coated glass surface, it is compatible with spin coating, doctor-blading, dip coating, screen printing, ink-jet printing, air-brushing, thermal treatments and vacuum thermal evaporation of organics or metals, as well as many other processing techniques. The material is commercially available at commodity scales, where the smallest available quantity is a 10 cm × 10 km roll. If the material itself is not compatible with a specific roll-to-roll processing step, it may be temporarily adhered to a thicker, more robust film (>100 μm) for processing, to be peeled off for shipping and used as desired. It is therefore compatible with roll-to-roll processing and ideal for modular manufacturing.

The ultrathin PLEDs presented in this work are the thinnest and most flexible electroluminescent devices to date. With a total thickness of only 2 μm, they can easily attain flexibility, with bending radii of 10 μm or smaller. As free-standing films, they can be crumpled under continuous operation. Their extreme flexibility renders them fully stretch-compatible, with demonstrated cyclic tensile strains up to 100%, with this number limited by the prestrain of the supporting elastomer and not by the PLED itself. The luminance output intensity is nearly display-compatible, and the output colour is red, and therefore suitable for RGB displays. Furthermore, the OLED technology itself is already the display standard for many mobile applications. This work represents a major step towards the realization of flexible, stretchable and surface-conforming electronics.

Methods

Device fabrication. Glass slides were cut to the appropriate size (2.5 × 2.5 cm) and cleaned by ultrasonic bath in Hellmanex detergent, followed by oxygen plasma treatment at 100 W for 5 min. A thin layer of PDMS (Sylgard 184 Silicone Elastomer, Dow Corning) was applied to the glass. A solution of 10:1 weight ratio PDMS to hardener, diluted 1:1 in hexane, was spin-coated at 8,000 r.p.m. for 60 s, and subsequently annealed at 150 °C for 30 min. The PET foil (Mylar 1.4 CW02) was then adhered to the surface by allowing the van der Waals forces to naturally form the flat film. Excess PET was trimmed from the surrounding area with shears. A dispersion of PEDOT:PSS was prepared from stock Clevios PH1000 with 5 vol% dimethyl sulphoxide and 0.5 vol% Zonyl FS-300 fluorosurfactant (Fluka). This formulation was spun onto the PET foil at 1,000 r.p.m. for 60 s and annealed at 120 °C for 30 min. The light-emitting polymer AnE-PV*stat* (synthesis described in detail elsewhere[17,19]) was dissolved in toluene (20 mg ml^{-1}), while stirring for 12 h at 90 °C. An optimal film thickness of 300 nm was prepared by spin-coating at 1,000 r.p.m. for 60 s with the solution and substrate both at 90 °C. The light-emitting polymer MDMO-PPV (purchased from Merck) was dissolved in toluene (8 mg ml^{-1}) and spin-coated at 1,500 r.p.m., resulting in 225-nm-thick films. Finally, 0.5 nm of LiF and 100 nm of Al were thermally evaporated through a shadow mask to form the electron injecting back electrode.

It should be noted that there are film thickness considerations related to the roughness of the ultrathin substrate. The PET foil is rough at the nanometre scale, with a listed root-mean square surface roughness of 26 nm and peak height of 700 nm. For this reason, a thick active layer (200–300 nm) was used in this work. With a thick active layer, substrates with eight pixels, each 3 mm × 6 mm in size, show excellent reproducibility, uniformity of emission and three or more orders of magnitude rectification at ±5 V driving bias. With thinner (50–100 nm) active layers, the resulting diodes show poor emission uniformity and excessive leakage current, indicating many pinholes. Thicker layers (~450 nm) resulted in devices with slightly lower radiance and slightly higher operating voltage due to increased resistivity.

Device characterization. Current–light–voltage characteristics were measured using an Agilent B1500 parameter analyser with two source meter units, one driving the PLED device and one measuring the photocurrent in a silicon photodiode. The quantitative electroluminescence spectra were measured using a Photo Research Spectrascan PR-655.

Compression and stretching. Elastomeric adhesive tape (3M VHB 4905) was placed between two clamps mounted on a compression jig, as shown schematically in Supplementary Fig. S3. A compression zone was defined using two rigid delimiters (red tape in Fig. 2; Supplementary Movies S2 and S3). Using a manually adjustable screw, the clamps were moved further apart to prestretch the elastomer to a desired length. The ultrathin PLED was then peeled away from the PDMS-coated glass support and applied to the prestretched elastomer by lightly pressing with a finger. Electrical contact was made with wires and silver paste in the area above the rigid delimiter. The device was then operated continually while the compression clamps were moved closer together, allowing the elastomer to relax to its unstrained position. The system could then be restretched to the same value of strain as originally specified, but further strain would result in disconnection or ripping of the ultrathin foil. At each stage of compression and stretching, the length of the PLED was used to determine the strain. As specified in Supplementary Fig. S3, the compression strain is defined as the change in length normalized to the fully extended (flat PLED) length, whereas the tensile strain is normalized to the fully compressed (relaxed elastomer) state. The total attainable compression and tensile strain is determined by the prestrain of the elastomer, here 100% tensile strain.

Further details of the experimental methods regarding compression and stretching, microstructure analysis and quantitative mechanical analysis are provided in the Supplementary Methods.

Received 16 November 2012; accepted 24 June 2013; published online 28 July 2013

References

1. Rogers, J. A., Someya, T. & Huang, Y. Materials and mechanics for stretchable electronics. *Science* **327,** 1603–1607 (2010).
2. Kim, D. H. *et al.* Dissolvable films of silk fibroin for ultrathin conformal bio-integrated electronics. *Nature Mater.* **9,** 1–7 (2010).
3. Kim, D. H. *et al.* Ultrathin silicon circuits with strain-isolation layers and mesh layouts for high-performance electronics on fabric, vinyl, leather, and paper. *Adv. Mater.* **21,** 3703–3707 (2009).
4. Timko, B. P. *et al.* Electrical recording from hearts with flexible nanowire device arrays. *Nano Lett.* **9,** 914–918 (2009).
5. Jung, I., Shin, G., Malyarchuk, V., Ha, J. S. & Rogers, J. A. Paraboloid electronic eye cameras using deformable arrays of photodetectors in hexagonal mesh layouts. *Appl. Phys. Lett.* **96,** 021110 (2010).
6. Jung, I. *et al.* Dynamically tunable hemispherical electronic eye camera system with adjustable zoom capability. *Proc. Natl Acad. Sci. USA* **108,** 1788–1793 (2011).
7. Sekitani, T. & Someya, T. Stretchable, large-area organic electronics. *Adv. Mater.* **22,** 2228–2246 (2010).
8. Cherenack, K., van Os, K. & van Pieterson, L. Smart photonic textiles begin to weave their magic. *Laser Focus World* 63–66 (April 2012).
9. Sekitani, T. *et al.* Stretchable active-matrix organic light-emitting diode display using printable elastic conductors. *Nature Mater.* **8,** 494–499 (2009).
10. Gray, D. S., Tien, J. & Chen, C. S. High-conductivity elastomeric electronics. *Adv. Mater.* **16,** 393–397 (2004).
11. Kim, K. S. *et al.* Large-scale pattern growth of graphene films for stretchable transparent electrodes. *Nature* **457,** 706–710 (2008).
12. Sekitani, T. *et al.* A rubberlike stretchable active matrix using elastic conductors. *Science* **321,** 1468–1472 (2008).
13. Lacour, S. P., Wagner, S., Huang, Z. & Suo, Z. Stretchable gold conductors on elastomeric substrates. *Appl. Phys. Lett.* **82,** 2404–2406 (2003).
14. Khang, D. Y., Jiang, H., Huang, Y. & Rogers, J. A. A stretchable form of single-crystal silicon for high-performance electronics on rubber substrates. *Science* **331,** 208–212 (2006).
15. Kim, D. H. *et al.* Stretchable and foldable silicon integrated circuits. *Science* **320,** 507–511 (2008).
16. Wagner, S. & Bauer, S. Materials for stretchable electronics. *MRS Bull.* **37,** 207–213 (2012).
17. Egbe, D. A. M. *et al.* Improvement in carrier mobility and photovoltaic performance through random distribution of segments of linear and branched side chains. *Mater. Chem.* **20,** 9726–9734 (2010).
18. Camaioni, N. *et al.* Electron and hole transport in an anthracene-based conjugated polymer. *Appl. Phys. Lett.* **101,** 053302 (2012).
19. Usluer, Ö. *et al.* Charge carrier mobility, photovoltaic and electroluminescent properties of anthracene-based conjugated polymers bearing randomly distributed side chains. *J. Polym. Sci. Polym. Chem.* **50,** 3425–3436 (2012).
20. Sierros, K. A., Morris, N. J., Ramji, K. & Cairns, D. R. Stress-corrosion cracking of indium tin oxide coated polyethylene terephthalate for flexible optoelectronic devices. *Thin Solid Films* **517,** 2590–2595 (2009).
21. Fortunato, E., Ginley, D., Hosono, H. & Paine, D. C. Transparent conducting oxides for photovoltaics. *MRS Bull.* **32,** 242–247 (2007).
22. Hekmatshoar, B. *et al.* Reliability of active-matrix organic light-emitting-diode arrays with amorphous silicon thin-film transistor backplanes on clear plastic. *IEEE Electron. Device Lett.* **29,** 63–66 (2008).
23. Steudel, S. *et al.* Design and realization of a flexible QQVGA AMOLED display with organic TFTs. *Org. Electron.* **13,** 1729–1735 (2012).
24. Rowell, M. W. *et al.* Organic solar cells with carbon nanotube network electrodes. *Appl. Phys. Lett.* **88,** 233506 (2006).
25. Yu, Z., Niu, X., Liu, Z. & Pei, Q. Intrinsically stretchable polymer light-emitting devices using carbon nanotube–polymer composite electrodes. *Adv. Mater.* **33,** 3989–3994 (2011).
26. Kaltenbrunner, M. *et al.* Ultrathin and lightweight organic solar cells with high flexibility. *Nat. Commun.* **3,** 770 (2012).
27. Lee, J. *et al.* Stretchable GaAs photovoltaics with designs that enable high areal coverage. *Adv. Mater.* **23,** 986–991 (2011).
28. Lipomi, D. J., Tee, B. C. K., Vosgueritchian, M. & Bao, Z. Stretchable organic solar cells. *Adv. Mater.* **23,** 1771–1775 (2011).
29. Wang, X., Hu, H., Shen, Y., Zhou, X. & Zheng, Z. Stretchable conductors with ultrahigh tensile strain and stable metallic conductance enabled by prestrained polyelectrolyte nanoplatforms. *Adv. Mater.* **23,** 3090–3094 (2011).
30. Graz, I. M., Cotton, D. P. J. & Lacour, S. P. Extended cyclic uniaxial loading of stretchable gold thin-films on elastomeric substrates. *Appl. Phys. Lett.* **94,** 071902 (2009).
31. Lipomi, D. J. & Bao, Z. Stretchable, elastic materials and devices for solar energy conversion. *Energy Environ. Sci.* **4,** 3314–3328 (2011).
32. Kim, T. I. *et al.* High-efficiency, microscale GaN light-emitting diodes and their thermal properties on unusual substrates. *Small* **8,** 1643–1649 (2012).
33. Kim, T. I., Kim, R. H. & Rogers, J. A. Microscale inorganic light-emitting diodes on flexible and stretchable substrates. *IEEE Photon. J.* **4,** 607–612 (2012).
34. Kim, H. *et al.* Unusual strategies for using indium gallium nitride grown on silicon (111) for solid-state lighting. *Proc. Natl Acad. Sci. USA* **108,** 10072–10077 (2011).
35. Kim, R. H. *et al.* Materials and designs for wirelessly powered implantable light-emitting systems. *Small* **8,** 2812–2818 (2012).
36. Hu, X. *et al.* Stretchable inorganic semiconductor electronic systems. *Adv. Mater.* **23,** 2933–2936 (2011).
37. Kim, P., Abkarian, M. & Stone, H. A. Hierarchical folding of elastic membranes under biaxial compressive stress. *Nature Mater.* **10,** 952–957 (2011).
38. Kim, J. B. *et al.* Wrinkles and deep folds as photonic structures in photovoltaics. *Nature Photon.* **6,** 327–332 (2012).
39. Zang, J., Zhao, X., Cao, Y. & Hutchinson, J. W. Localized ridge wrinkling of stiff films on compliant substrates. *J. Mech. Phys. Solids* **60,** 1265–1279 (2012).
40. Ebata, Y., Croll, A. B. & Crosby, A. J. Wrinkling and strain localizations in polymer thin films. *Soft Matter* **8,** 9086–9091 (2012).
41. Gregg, B. A. & van de Lagemaat, J. Solar cells: folding photons. *Nature Photon.* **6,** 278–280 (2012).
42. Heeger, A. J., Sariciftci, N. S. & Namdas, E. B. *Semiconducting and Metallic Polymers* 167–168 (Oxford Univ. Press, 2010).

Acknowledgements

The authors thank Pütz GmbH & Co. Folien KG for the ultrathin substrates. This work was partially funded by the ERC Advanced Investigators Grant 'SoftMap' and the JST–ERATO Someya Bio-Harmonized Electronics grant. The authors are grateful to the Austrian FWF for financial support through the Wittgenstein Award. N.S.S. and M.S.W. acknowledge financial support from the J-RISE (JST) Yamagata University–Johannes Kepler University collaboration. D.A.M.E. and C.U. acknowledge the Deutsche Forschungsgemeinschaft (DFG) for financial support in the framework of SPP 1355. S.A. acknowledges support from the African Network for Solar Energy (ANSOLE) for enabling her stay at LIOS under the framework of the ANEX-Program. The authors thank J. Reeder, P. Stadler and P. Denk for their contributions.

Author contributions

D.A.M.E. and C.U. conceived and synthesized the light-emitting polymer. M.S.W., M.K., E.D.G., K.G. and S.A. fabricated and characterized devices. G.K., K.G. and I.G. processed ultrathin substrates and assisted with device demonstrations. M.S.W., M.K. and S.B. wrote the manuscript and prepared figures, with contributions from all authors. M.C.M. and Z.M. performed the quantitative mechanical analysis. Ta.S., Ts.S., M.C.S., S.B. and N.S.S. supervised the project and advised on device optimization.

Additional information

Supplementary information is available in the online version of the paper. Reprints and permissions information is available online at www.nature.com/reprints. Correspondence and requests for materials should be addressed to M.S.W.

Competing financial interests

The authors declare no competing financial interests.